frontiers | Frontiers in Environmental Science

TYPE Original Research
PUBLISHED 20 October 2022
DOI 10.3389/fenvs.2022.1043638

OPEN ACCESS

EDITED BY
Shaoda Liu,
Beijing Normal University, China

REVIEWED BY
Ni Maofei,
Guizhou Minzu University, China
Sujay Raghavendra Naganna,
Siddaganga Institute of Technology, Tumakuru, India

*CORRESPONDENCE
M. Peipoch,
mpeipoch@stroudcenter.org

SPECIALTY SECTION
This article was submitted to Freshwater Science,
a section of the journal
Frontiers in Environmental Science

RECEIVED 13 September 2022
ACCEPTED 06 October 2022
PUBLISHED 20 October 2022

CITATION
Bacmeister E, Peck E, Bernasconi S, Inamdar S, Kan J and Peipoch M (2022), Stream nitrogen uptake associated with suspended sediments: A microcosm study.
Front. Environ. Sci. 10:1043638.
doi: 10.3389/fenvs.2022.1043638

Stream nitrogen uptake associated with suspended sediments: A microcosm study

Eva Bacmeister[1], E. Peck[1], S. Bernasconi[2], S. Inamdar[1], J. Kan[2] and M. Peipoch[2]*

[1]Plant and Soil Sciences, University of Delaware, Newark, DE, United States, [2]Stroud Water Research Center, Avondale, PA, United States

Despite significant advances in our understanding of nitrogen (N) removal pathways along river networks, the role of water column processes remains largely understudied. This knowledge gap not only limits our capacity to determine N transport and retention in mid-to-large rivers but also hampers our understanding of N removal processes in smaller streams during stormflow conditions, in which significant increases in suspended sediment concentrations (SSC) typically occur. High SSC in the water column can provide abundant substrate for microbial growth and water column N uptake. However, storms of different size mobilize different quantities of sediment of varying properties and sizes, which can ultimately modulate water column N uptake rates in the stream during stormflows. To assess water column N uptake associated with suspended sediment particles of different sources and sizes, we quantified assimilatory and dissimilatory N uptake rates in a set of microcosms representing a gradient of sediment properties (organic matter, N content, and microbial activity) and surface area (fine vs. coarse size) availability. Water column assimilatory uptake (U_{sed}) ranged from 12.7 to 187.8 μg N [g sediment]$^{-1}$ d^{-1} across all sediment sources and size fractions, and was higher on average than denitrification rates (DN_{sed}) in agricultural and stream bank sediments but not in streambed sediments (mean DN_{sed} = 240.9 ± 99 μg·N [g sediment]$^{-1}$·d^{-1}). Sediment-bound C in suspended sediment varied among sediment sources and was directly related to U_{sed} rates, but not to DN_{sed} rates, which were less predictable and more variable. Overall, our results showed a positive nonlinear relationship between water column N uptake and SSC, while indicating that water column N uptake may scale differently to SSC depending on sediment source, and to a lesser degree, particle size. Because low, moderate, and large storms can mobilize different quantities of sediment in the watershed of different sources and sizes, it is likely that storm size will ultimately modulate the contribution of water column uptake during storm events to whole-reach N retention.

KEYWORDS

stream, nitrogen, suspended sediment, uptake, denitrification

Introduction

Global nitrogen (N) export from watersheds has exceeded more than twice its preindustrial value due to modern human activities (Schlesinger, 2009), with streams of many regions experiencing up to a 5-fold increase in total N concentrations (Dodds and Smith, 2016). In North America, only a quarter of the monitored streams and rivers are currently showing long-term decreasing trends in N concentrations (Shoda et al., 2019), which indicates that nutrient enrichment remains a major threat to the ecological integrity of running waters. The improved management of excessive N loads requires both a reduction of anthropogenic N inputs and a more comprehensive understanding of N removal pathways along river networks and among different streamflow conditions (Wollheim et al., 2017, Wollheim et al., 2018). Previous research has focused largely on benthic N removal in headwater streams during baseflow, while much less is known about the role of water column N removal in larger streams or during stormflow conditions.

Most of the benthic N uptake in headwater streams is associated with biological assimilation and storage, *aka* assimilatory N uptake (Peterson et al., 2001; Arango et al., 2008), a temporary N retention that can last from hours to days (Peipoch et al., 2014; Tank et al., 2018). The remainder of benthic N uptake is associated with dissimilatory uptake, including denitrification, a major pathway by which N is permanently removed from aquatic ecosystems through anaerobic microbial respiration (Craig et al., 2008; Mulholland et al., 2009). Denitrification can occasionally account for more than 40% of benthic nitrate uptake in headwater streams (Mulholland et al., 2009). However, N uptake also occurs in the water column of streams of varying size (Reisinger et al., 2015, Reisinger et al., 2016), but the paucity of water column uptake measurements limits our understanding of the relative contribution of assimilatory and dissimilatory pathways to water column N uptake and the major controlling factors of these pathways. Previous studies have shown that water column N uptake is strongly related to suspended sediment concentration, particle size, and nutrient availability (Jia et al., 2016; Reisinger et al., 2021). In particular, large surface area generated by high concentrations of fine particles in the water column and associated organic matter can provide abundant substrate for microbial growth and N uptake (Liu et al., 2013; Jia et al., 2016), including anaerobic processes such as denitrification since suspended particles can retain anoxic microsites (Jia et al., 2016; Xia et al., 2017, Xia et al., 2018). Results to date indicate a strong dependence of water column N uptake rates on suspended sediment concentration. While some rivers can have high concentrations of suspended sediments during baseflow conditions (e.g., 20 $g{\cdot}L^{-1}$ in Xia et al., 2017), most streams and mid-size rivers only carry high suspended sediment loads during and immediately after storm events, highlighting the importance of better understanding N uptake processes during stormflow conditions.

Stormflows cause significant increases in suspended sediment concentrations of small-to mid-order streams (< 4th order; Cashman et al., 2018; Noe et al., 2020). During and after significant storm events, suspended sediment particles in relatively small streams may provide a comparable amount of water-sediment interface to that in the streambed, akin to the increase in bioavailable surface area associated with suspended sediment when streams become rivers (Gardner and Doyle, 2018). In fact, much like the longitudinal transition from small streams to large rivers, storm events cause short-term increases in water depth, suspended sediment concentrations, and sediment-bound nutrients (Wood and Armitage, 1997) that can promote water column uptake at event scales even in headwater networks. Other factors may also contribute to the potential nutrient uptake capacity in the water column during storm events. For instance, anthropogenic land use can play a role in the quantity and character of particles in suspension (Gellis and Mukundan, 2013; Gellis and Gorman-Sanisaca, 2018). Low intensity summer thunderstorms have been associated with resuspension of sediment particles originating from the stream channel (e.g., stream bed and banks), while larger storm events bring a greater contribution of particles from the surrounding landscape (Karwan et al., 2018; Jiang et al., 2020). Moderate storm events following freeze-thaw cycles in the winter have been implicated in stream bank erosion, yielding significant fluxes of fine sediment particles from stream banks (Inamdar et al., 2018). Overall, suspended sediment particles from different sources can vary in grain size and nutrient content (Jiang et al., 2020; Lutgen et al., 2020), which may ultimately affect the potential rates of water column N uptake during and after storm events.

Here, we used a microcosm approach to simulate suspended sediment concentrations in streams during storm events of different magnitude. Our goal was to assess how the source, size, and concentration of suspended sediments influence water column N uptake. Sediment particles of different sources and size generated a gradient of sediment properties (organic matter, N content, and microbial activity) and surface area availability. In particular, we evaluated fine (<63 μm) and coarse (63–2000 μm) fractions of three of the most common sediment sources that are mobilized by storm events of varying intensity in the Mid-Atlantic region of the US: Streambed, stream bank, and agricultural soils (Gellis and Noe, 2013; Cashman et al., 2018; Jiang et al., 2020; Noe et al., 2020). We hypothesized that fine fractions of stream bank and upland agricultural sources will result in higher water column N uptake due to the greater surface area and sediment-bound nutrient content (e.g., Jiang et al., 2020) associated with their dominance of fine sediment particles. In the microcosms, we experimentally manipulated suspended particle concentrations (up to 5,000 $mg{\cdot}L^{-1}$) for each size fraction and sediment source, and measured both

assimilatory N uptake and denitrification rates in each microcosm using ^{15}N tracer methods.

Materials and methods

Sediment sampling and characterization

In the summer of 2021, we collected sediments at three different locations (one for each sediment source) within the White Clay Creek watershed, Pennsylvania, United States. The White Clay Creek (WCC) is a temperate third order stream of characteristic conditions in the Piedmont physiographic province of southeastern Pennsylvania. Mean annual precipitation and temperature in WCC are 1,190 mm and 11.7°C, respectively (period 2009–2020). At the location of sediments collection, the stream drains a 7-km two watershed dominated by pasture/hay (48%), deciduous forest (19%), cultivated crops (17%) and woody wetlands (4%) with a mostly closed-canopy stream network (~65% of forested riparian areas). We collected streambed and stream bank sediments from the East Branch of WCC and surface soils (top 15 cm; 39°51′32.5″N 75°47′00.6″W) from agricultural fields located upland of this stream branch (39°51′38.5″N 75°46′50.3″W). The location of sediment collection was partially guided by our previous sampling described by Lutgen et al. (2020). At each location, sediment was collected from three different sites within the location area and composited in a single sample. We collected, homogenized, and transported the necessary amount of sediment (500 g) for microcosm experiments to the laboratory, where it was processed immediately and kept in the dark overnight at 4°C. In all cases, sediment collection and the starting of each microcosm experiment occurred in less than 24 h. Prior to each sediment collection for the microcosm study, we took sterile samples of each sediment source for the characterization of denitrifying *nosZ* genes (clades I and II) abundances; these samples were collected in WhirlPaks and immediately stored at 0°C. We also collected additional samples to characterize the particle size distribution of each sediment source by volume and surface area (assuming spherical geometry of all particle sizes) using a Beckman Coulter LS 13 320 particle size analyzer.

In the laboratory, we first separated sediments from each source into clay/silt (<63 μm) and sand (63–2000 μm) size fractions by sequentially wet sieving the collected sediments through 2000 and 63 μm sieves using stream water from WCC. Then, we vacuum filtered all the sieved water in the previous step using 0.70-μm pore size glass fiber filters (Whatman filter Sigma-Aldrich, Missouri, United States) to compile <63 μm particles while keeping the filtered water for the preparation of the microcosm experiments. This was done to ensure that microbes dislodged during the wet sieving process were added to the microcosms (Jia et al., 2016). The sieving process was repeated until sufficient sediment and stream water were collected for the execution of each microcosm experiment. Prior to the microcosm incubations, we subsampled the 0.70-μm filtered water used in the sieving process of each sediment source for the analysis of dissolved organic carbon (DOC) and nitrate ($N\text{-}NO_3^-$) concentrations. DOC concentrations were determined using an Aurora 1030 W TOC Analyzer (Oceanographic Int., College Station, Texas, United States) and chemical oxidation (Menzel and Vaccaro, 1964). The concentrations of $N\text{-}NO_3^-$ were determined by discrete colorimetric analysis using an AQ300 discrete analyzer (SEAL Analytical, Wisconsin, United States) following standard procedures (APHA 2017).

For the characterization of denitrifying *nosZ* genes in each sediment source, the genomic DNA was extracted using DNeasy PowerSoil Pro Kit (Qiagen, Germantown, MD) and the *nosZ* genes were quantified with qPCR on a QuantStudio TM three system with Analysis Software v1.5.1 (Thermo Fisher Scientific, Waltham, WA). For *nosZ* clade I the qPCR was performed using the primers *nosZ* 1840F(CGCRACGGCAASAAGGTSMSSGT) and *nosZ*2090 R (CAKRTGCAKSGCRTGGCAGAA) (Henry et al., 2006). 20 μl reactions contained 1X Power Up SYBR Green Master Mix (Applied Biosystems, Waltham, MA), 0.5 μM each primer, and 0.6 mg/ml BSA (Invitrogen, Waltham, MA). The protocol is as follows: An initial 50°C for 2 min and 95°C for 10 min, followed by six cycles of 95°C for 15 s, 65°C for 30 s, 72 for 30 s, and 80°C for 15 s, then 45 cycles of 95°C for 15 s, 60°C for 30 s, 72 for 30 s, and 80°C for 15 s, ending with a melt curve step. The quantification of nosZ clade II was performed using the primers *nosZ*IIF (CTIGGICCIYTKCAYAC) and *nosZ*IIR (GCIGARCARAAITCBGTRC) (Jones et al., 2013). 20 μl reactions contained 1X Power Up SYBR Green Master Mix, two uM each primer, and 0.5 mg/ml BSA. The protocol was as follows: an initial 50°C for 2 min and 95°C for 5 min, followed by 45 cycles of 95°C for 20 s, 52 for 35 s, and 72 for 1 min 10 s, followed by a melt curve step. Each qPCR run contained a standard curve of 10X serial dilutions of gBlocks Gene Fragments from Integrated DNA Technologies (Coralville, IA), and the gene quantification was standardized to gene copy numbers per Gram of soil.

Suspended sediment microcosm incubations

We quantified nitrate uptake rates (assimilatory and denitrification) associated with different suspended sediment sources, size, and concentrations using a three-level factorial design of microcosm incubations. Microcosms consisted of a modified Kimble 250 ml wide-mouth media bottles with screw caps with rubber septa installed. To generate a gradient of suspended sediment concentrations (SSC), we individually weighed aliquots of sediment from each source and size class

to generate four different treatment levels of SSC: 500, 1,000, 2,500, and 5,000 mg·L^{-1}. The selected SSC range (0.5–5 g·L^{-1}) is similar to that observed in WCC for storm events of varying size (Jiang et al., 2020). Unfortunately, targeted concentrations were difficult to pinpoint precisely due to the unknown water content contribution to wet sediment weight, and despite our best efforts, we ended up with a continuous gradient of SSC across the 12 replicates per sediment source and size. Consequently, SSC was included as a continuous variable in our data analysis with comparable ranges across sediment source and size treatments: 130–5,408 mg·L^{-1} for streambed, 177–6,216 mg·L^{-1} for stream bank, and 224–5,281 mg·L^{-1} for agricultural sediments. We replicated each treatment by triplicate (sediment source × particle size × concentration) making a total of 75 microcosms including sediment-free blanks bottles. After sediment aliquots were added, we poured 250 ml into each microcosm using the stream water previously used to separate sediment size fractions. We placed a magnetic stir bar in each microcosm and then added 1 ml of a 796 mg·L^{-1} solution of $Na^{15}NO_3^-$ specifically prepared to generate less than a 5% increase of the N-NO_3^- concentration in each microcosm. We capped the microcosms and evacuated (3 min) and flushed with He gas (1 min) by inserting tubing with syringe needles attached into the septa of each microcosm chamber (Dodds et al., 2017), repeating the evacuating and flushing cycle three times prior to the beginning of each incubation.

Then, microcosms were placed on magnetic stir plates within an incubator set to 25°C. We set the stir plates to 360 rpm to ensure particles remained in suspension during the incubation period (Jia et al., 2016), and then closed the incubator to keep chambers in the dark. We sampled dissolved gas at 4 and 24 h after the start of incubation, using a gas-tight syringe (Hamilton 25 ml Model 1025TLL) to sample 12 ml of gas from each chamber into 12 ml pre-evacuated Exetainers (Labco Ltd., High Wycombe, United Kingdom). The timing of gas sample collection was determined after conducting preliminary microcosm incubations that showed consistent linear increases of N_2 and N_2O mass between 4 and 24 h. Gas samples were analyzed for $\delta^{15}N$ of N_2, and N_2O *via* IRMS (ThermoScientific Delta V Plus) at the University of California-Davis Stable Isotope Facility.

At the end of incubations, we carried out a suite of additional analyses of the sediment and water in each microcosm. These included SSC, organic matter (OM) content, C and N content, and $\delta^{15}N$ signatures of suspended sediments. Sediment samples for SSC analysis were collected on pre-weighted FVF glass fiber filters, oven-dried at 60°C for 72 h, and weighed on a Sartorius (Goettingen, Germany) MC1 analytical balance. OM samples were oven-dried at 60°C for 72 h, weighed on a Sartorius (Goettingen, Germany) MC1 analytical balance, combusted at 500°C for 5–6 h, and reweighed for calculation of dry mass and ash-free dry mass (e.g., OM). Sediment samples for elemental and isotopic analyses of C and N were collected on pre-weighted glass fiber filters, encapsulated in tins, and sent to the UC Davis Stable Isotope Facility (California, United States). The C and N content (as a percentage of total dry mass) and ^{15}N isotope signatures were determined using a PDZ Europa ANCA-GSL elemental analyzer interfaced to a PDZ Europa 20–20 isotope ratio mass spectrometer (Sercon, Cheshire, United Kingdom). We also analyzed filtered water from each microcosm for DOC and N-NO_3^- concentrations using the same methodology described above.

Uptake calculations and data analysis

We calculated rates of assimilatory uptake by total suspended sediment in each microcosm following Mulholland et al. (2000), using the increase in tracer ^{15}N mass associated with suspended OM ($^{15}N_{susp\text{-}OM}$) at the end of the incubation and the tracer ^{15}N:^{14}N ratio in the microcosm NO_3^- ($^{15}N\text{-}NO_3^-$) as follows:

$$U_{micro} = \frac{^{15}N_{susp-OM}}{^{15}N - NO_3 * \Delta t},$$

where U_{micro} is the microcosm-specific rate of assimilatory uptake (μg N d^{-1}); $^{15}N_{susp\text{-}OM}$ is the background-corrected ^{15}N mass associated with suspended OM; and Δt is the incubation time. We calculated $^{15}N_{susp\text{-}OM}$ in μg ^{15}N $microcosm^{-1}$ as the product of the ^{15}N molar fraction, N %, and OM mass in each microcosm and subtracting from it the background ^{15}N mass. We estimated $^{15}N\text{-}NO_3^-$ using background N-NO_3^- concentrations in each microcosm and the amount of tracer $^{15}N\text{-}NO_3^-$ added assuming a background ^{15}N:^{14}N ratio equal to 0.0036765 (that is $\delta^{15}N\text{-}NO_3^- = 0‰$).

Denitrification rates by total suspended sediment in each microcosm were calculated from the production rate of $^{29}N_2$ (r_{29}) and $^{30}N_2$ (r_{30}) following calculations for total denitrification rate associated with sediments described by Nielsen (1992) as follows:

$$DN_{micro} = (r_{29} + 2 * r_{30}) * \frac{r_{29}}{2 * r_{30}},$$

where DN_{micro} is the microcosm-specific denitrification rate (μg·N·d^{-1}). Prior to this calculation, r_{29} and r_{30} were calculated from the difference in $^{29}N_2$ and $^{30}N_2$ (in moles) between 4 and 24 h after the start of incubation. We determined the molar amount of $^{29}N_2$ and $^{30}N_2$ in each microcosm and time by multiplying total N_2 molar amount for the molar fraction of $^{29}N_2$ and $^{30}N_2$, respectively. Total molar N_2 amount was determined as the sum of N_2 moles in the water and gas phase using the specific Bunsen coefficients for N_2 according to the incubation temperature (Weiss, 1970; Dodds et al., 2017). Finally, we converted U_{micro} and DN_{micro} rates to sediment-specific rates (U_{sed} and DN_{sed} as μg·N [g sediment]$^{-1}$·d^{-1}) by dividing them for the dry weight of suspended sediment in each microcosm.

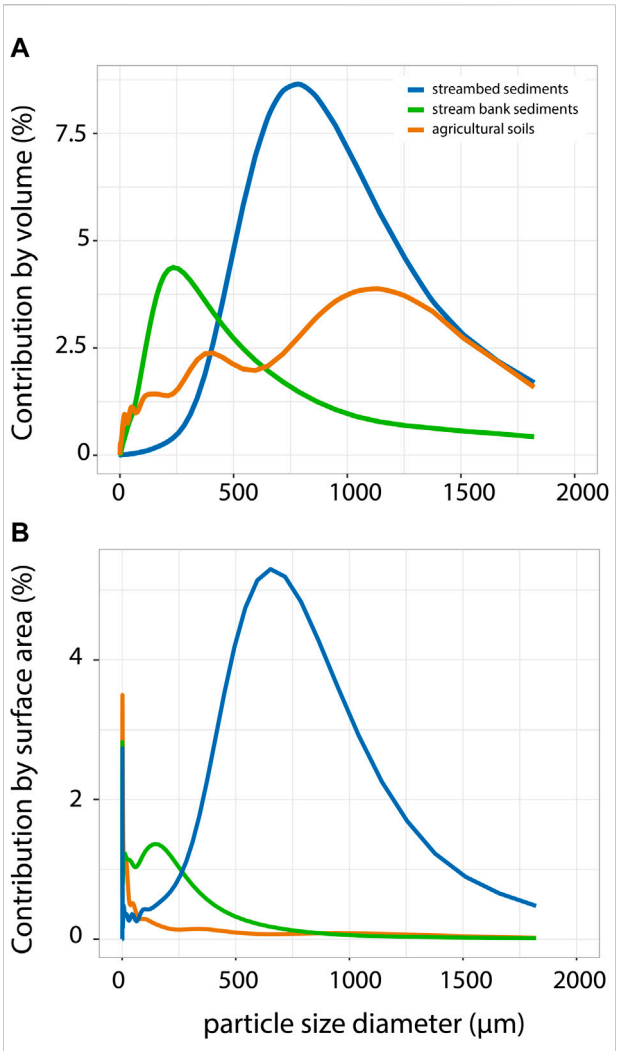

FIGURE 1
Sediment size distribution by volume **(A)** and surface area **(B)** of each sediment source. The top of the curve corresponds to the median particle diameter or surface area, for which the percentage of particles with diameters or area smaller and larger than this are 50%.

Statistical analysis of the differences in sediment properties and N uptake rates among sediment sources and sizes were addressed using non-parametric approaches with $\alpha = 0.05$. Specifically, we performed Kruskal–Wallis followed by unpaired Wilcoxon tests for comparisons among multiple sources and particle size and to address comparisons between two groups, respectively. Effects of sediment source, size and concentration on both assimilatory uptake and denitrification rates were assessed using simple linear regressions and Analysis of Covariance (ANCOVA) on $\log_{10}$-transformed variables with $\alpha = 0.05$. When necessary, appropriate constants were added to ensure positive values before transformation to meet linear model assumptions. ANCOVA models on assimilatory uptake and denitrification were performed separately, with sediment source and size as independent factors and SSC as a covariate. All statistical analyses were performed in the R environment (R Core Team, 2013).

Results

Biogeochemical properties and size across sediment sources

Beckman-Coulter particle size analysis indicated that for both surface area and volume, contributions of sand particles (> 63 μm) to stream bed sediment were significantly greater than for stream bank or agricultural sediments (Figure 1). By volume, agricultural sediments showed a more variable distribution than streambed and stream bank sediments (Figure 1A). Particle size distribution of streambed sediments was almost normally distributed and centered on 600 μm (Figure 1A), while the most common size in stream bank sediments (d50) was 235.6 μm with a strongly right-skewed distribution indicating a low presence of very large particles (Figure 1A). By surface area, all sediment sources showed a significant peak in the clay/silt fraction (<63 μm; Figure 1B), indicating the important role of fine sediments in providing available substrate area for microbial biota.

We found similar organic matter (OM) content on average among the sediment sources but substantial variation within each of them, with higher mean OM in the sand fraction of each sediment source (Table 1; Figure 2A). Carbon and nitrogen content (%C and % N) in suspended sediment were highest in agricultural sediments, intermediate in stream bank, and lowest in stream sediment (Table 1). For agricultural sediments, mean %C and %N in the sand fraction nearly doubled those of the clay/silt fraction (Table 1; Figure 2B); whereas both stream bank and streambed sediments showed the opposite pattern (Figure 2C), and a particularly low %N in the sand fraction of streambed sediment that resulted in mean C:N ratio for this source and size being more than tenfold higher than any other value (Table 1). Mean concentrations of both nitrate and DOC were much higher in microcosms with agricultural sediments than in those with stream bank or streambed sediments (Table 1). In contrast, mean concentrations of N-NO_3^- and DOC varied little between size fractions of each sediment source (Table 1). Only clade I *nosZ* genes were detected in our samples, and the results showed that agricultural sediments contained a larger content of denitrifying *nosZ* genes than stream bank and streambed sediments (Table 1). Overall, differences in mean values of the measured sediment properties (OM, %C, %N, and *nosZ*) were greater among sources than between size fractions examined within each source (Table 1; Figure 2).

Variation in water column nitrogen uptake

Water column assimilatory uptake (U_{sed}) varied over an order of magnitude for each sediment source, with mean U_{sed}

TABLE 1 Biogeochemical properties of sediment sources and size fractions, including organic matter content (OM), C content in OM (C), N content in OM (N), molar C-to-N ratio (molar C:N), concentration of nitrogen-nitrate (NO_3-N), concentration of dissolved organic C (DOC), and number of denitrifying nosZ genes per sediment mass (nosZ genes). Values in bold show the means +/− SEM based on all replicates for each sediment type (N = 12), except for nosZ genes. Means +/− SEM for associated size fractions (N = 6) within each sediment type are listed below bolded value. Mean values within a column with unique superscripts are significantly different ($p < 0.05$) following Kruskal–Wallis and unpaired Wilcoxon tests.

Sediment source and size	OM (%)	C (%)	N (%)	molar C:N	NO_3-N (μg·L^{-1})	DOC (mg·L^{-1})	*nosZ* genes (10^3 copies [g·sed]$^{-1}$)
agricultural	**14.3 ± 0.6**	**4.2AB ± 0.4**	**0.4A ± 0.03**	**12.3A ± 0.8**	**4.46A ± 0.15**	**5.7A ± 0.04**	**20,617 ± 2,143**
Sand	13 ± 0.5	5.2 ± 0.6	0.4 ± 0.06	14.5 ± 1.3	4.66 ± 0.11	5.6 ± 0.06	
clay/silt	15.5 ± 1.1	3.1 ± 0.1	0.4 ± 0.01	10.1 ± 0.3	4.27 ± 0.27	5.8 ± 0.05	
streambank	**11.5 ± 1.2**	**4.4A ± 0.3**	**0.4A ± 0.04**	**23.8B ± 6.9**	**2.83B ± 0.12**	**1.9B ± 0.04**	**661.4 ± 65.6**
sand	8.6 ± 1.8	4.3 ± 0.6	0.4 ± 0.08	34.5 ± 13.4	2.79 ± 0.12	1.9 ± 0.07	
clay/silt	14.3 ± 1.2	4.5 ± 0.2	0.4 ± 0.03	13 ± 0.3	2.87 ± 0.2	1.9 ± 0.05	
streambed	**15.4 ± 2.2**	**3.2B ± 0.2**	**0.2B ± 0.03**	**71.5C ± 17.3**	**3.74C ± 0.04**	**2B ± 0.05**	**16.6 ± 3.1**
sand	13.9 ± 1.7	3.4 ± 0.4	0.03 ± 0.01	130.5 ± 24.7	3.6 ± 0.03	1.8 ± 0.03	
clay/silt	17 ± 4.1	3.2 ± 0.2	0.3 ± 0.01	12.5 ± 0.3	3.9 ± 0.05	2.2 ± 0.05	

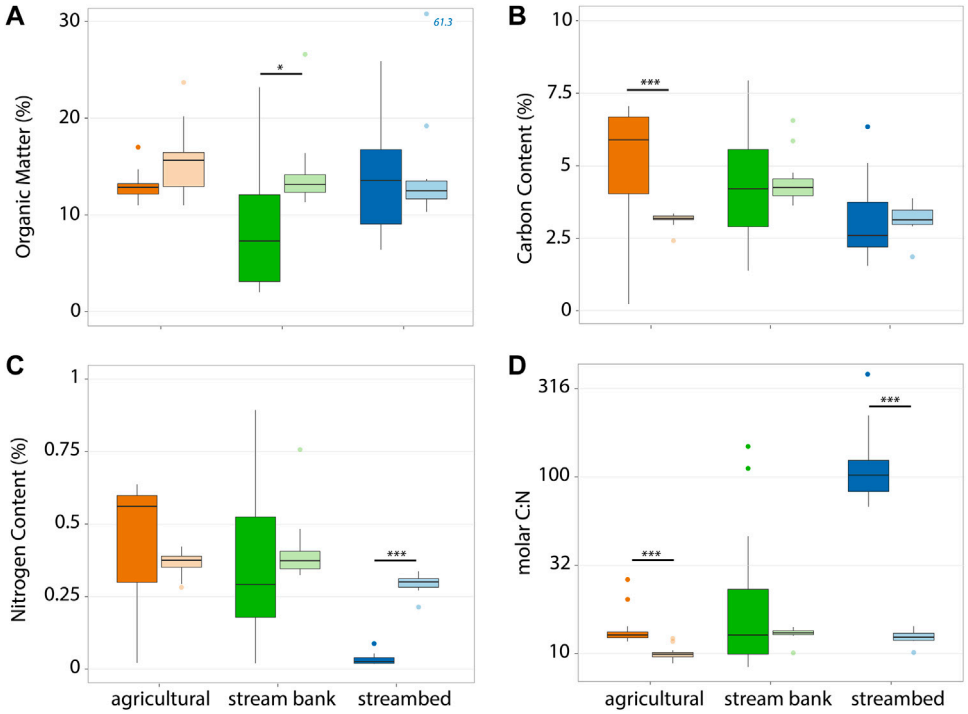

FIGURE 2
Box-plots of organic matter **(A)**, C content **(B)**, N content **(C)**, and M C:N ratio **(D)** for agricultural (orange), stream bank (green), and streambed (blue) sediments. Data for each size fraction are represented in dark and light colors for sand and silt/clay, respectively. Within each sediment source, significantly different values for each size fraction (unpaired Wilcoxon tests following significant Kruskal–Wallis) are indicated as: [blank] $p > 0.05$; *$p < 0.05$; **, $p < 0.01$; ***$p < 0.001$.

from each size fraction ranging from 12.7 to 56.6 μg·N [g sediment]$^{-1}$·d^{-1} for streambed sediments, from 30.1 to 187.8 μg·N [g sediment]$^{-1}$ d^{-1} for stream bank sediments, and from 114.2 to 118 μg·N [g sediment]$^{-1}$·d^{-1} for agricultural sediments (Figure 3A). U_{sed} was higher in clay/silt sediments from the streambed than in sand, and the opposite for stream

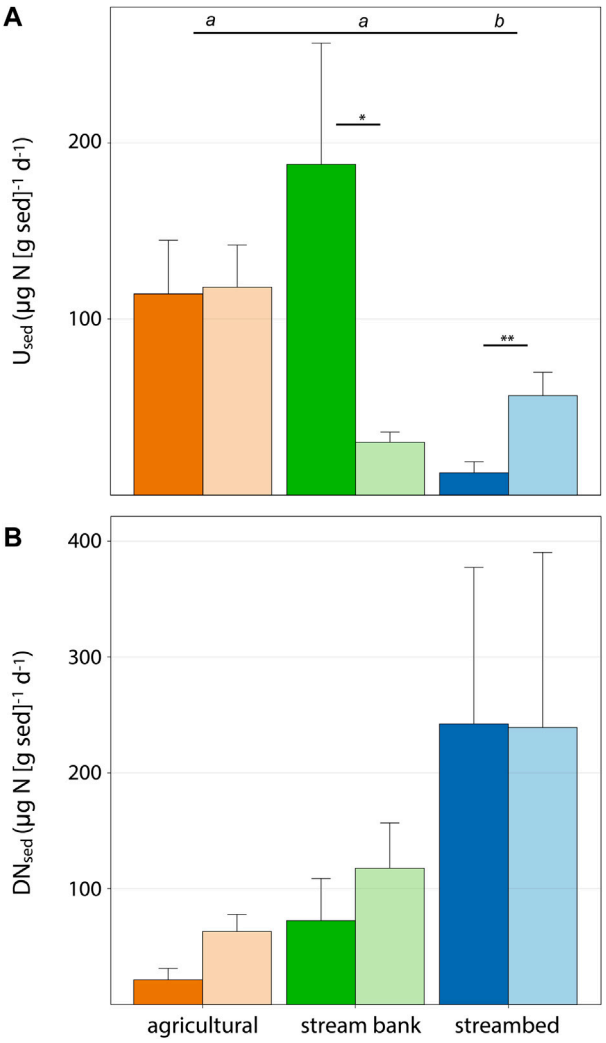

FIGURE 3
Sediment-specific rates of assimilatory uptake **(A)** and denitrification **(B)** for each sediment source and size. Bar height and error bars correspond to mean and SEM values, respectively (N = 12). Color legend is consistent with Figure 2. Size fractions are represented in dark and light colors for sand and silt/clay, respectively. Among sediment sources, bars with unique letters on the top of each panel are significantly different (unpaired Wilcoxon tests following significant Kruskal–Wallis). Within each sediment source, significantly different values between size fractions are indicated as: [blank] $p > 0.05$; *$p < 0.05$; **, $p < 0.01$; ***$p < 0.001$.

banks sediments (Figure 3A). On average, U_{sed} was significantly lower in streambed sediments than in agricultural and stream bank sediments. In contrast, the mean denitrification rate (DN_{sed}) in streambed sediments was higher compared to agricultural and bank sources for both clay/silt and sand fractions (Figure 3B). Water column DN_{sed} also varied over two orders of magnitude for each sediment source, with DN_{sed} rates in streambed sediments being more variable than DN_{sed} in the other two sediment sources (Figure 3B). Specifically, streambed sediments showed the highest DN_{sed} rates (1.7 mg·N [g sed]$^{-1}$·d^{-1}) and a similar number of non-detectable DN_{sed} rates compared to the other sediment sources (Figure 3B). Overall, we found similar or greater N uptake rates (U_{sed} and DN_{sed}) in the microcosms containing clay/silt than in those filled with sand, but this pattern was not consistent across all sediment sources and showed limited statistical significance (Figure 3B).

Controls on water column nitrogen uptake

Sediment %C was positively correlated to U_{sed} ($r = 0.37$, $p < 0.01$), but not to DN_{sed}, when considering all sediment sources and size fractions. More specifically, we found that the relationship between sediment %C and U_{sed} was positive and of identical effect size across the three sediment sources (Figure 4A), whereas only DN_{sed} rates in streambed sediments showed a positive relationship with sediment %C (Figure 4B). Similarly, at the microcosm scale, the effects of increasing SSC were much more apparent on assimilatory N uptake (U_{micro}) than on denitrification rates (DN_{micro}; Figure 5). U_{micro} showed positive and significant log-log relationships with increasing SSC of clay/silt and sand particles for both agricultural and stream bank sediments (Figures 5A,C). The exponents of the U_{micro}-SSC relationships were very similar between these two sediment sources and slightly higher for the sand fraction (Figures 5A,C). Unlike for agricultural and stream bank sediments, U_{micro} in streambed sediments were not related to increasing SSC of either clay/silt or sand particles (Figure 5E). DN_{micro} rates were only significantly related to increasing SSC of stream bank silt (Figures 5B,D,F). Overall, individual relationships between SSC and water column N uptake changed abruptly when comparing streambed sediments to the other sediment sources, indicating differences in how water column N uptake scales with SSC depending on sediment source. In concordance, ANCOVA models showed significant, positive effects of both sediment source and SSC on assimilatory uptake rates, but not for denitrification (Table 2). For assimilatory uptake, ANCOVA ($R^2 = 0.72$) results showed that the slopes of the uptake *versus* SSC relationships were significantly different among the sediment sources, and particularly between streambed and the other two sources (Table 2).

Discussion

Our microcosm approach attempted to recreate the turbulent and turbid conditions in streams during stormflows to estimate water column N uptake associated with sediment of different sources, and which are mobilized by storm events of different

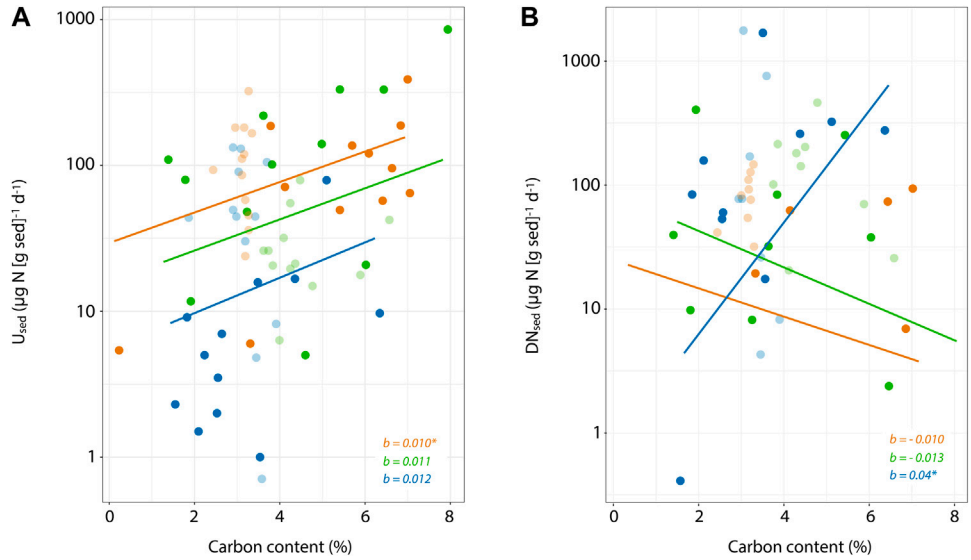

FIGURE 4
Relationships of sediment C content with sediment-specific assimilatory uptake rates **(A)** and denitrification rates **(B)** among sediment sources. Note vertical axis is $\log_{10}$ transformed and that color legend is consistent with previous figures. Slope lines were computed including data from both size fractions for each sediment source, and their values and significance ([blank] $p > 0.05$; *$p < 0.05$; **, $p < 0.01$; ***$p < 0.001$) are indicated in each panel. DN_{sed} values below our detection limit are omitted in the plot but were considered for the slope calculation.

intensity. We successfully measured assimilatory and dissimilatory N uptake across a range of suspended sediment concentrations that are characteristic of low (<0.3 mg·L^{-1}), to moderate (0.3–2 mg·L^{-1}), to very large (>2 mg·L^{-1}) storms in the Mid-Atlantic region. Sediment-bound C in suspended sediment varied among sediment sources and was directly related to assimilatory N uptake rates, but not to denitrification rates, which were less predictable and more variable. Like others before (Liu et al., 2013; Xia et al., 2017; Reisinger et al., 2021), we generally found a positive and significant relationship between the concentration of suspended sediments and water column uptake; however, our results also showed that water column N uptake scaled differently to suspended sediment concentrations depending on sediment source, and to a lesser degree, particle size. These results are complementary to previous work quantifying whole-reach N retention during stormflow conditions. By comparing predicted and observed NO_3^- fluxes in a watershed's outlet, Wollheim et al. (2017) estimated 65% net retention of nitrate at the network scale during small storm events and no net retention during large storms. They explained the decline in network-scale N retention with storm size due to NO_3^- fluxes increasing at a faster rate (log-log slope >1) with storm runoff at the mouth of the watershed than in its headwaters (log-log slope ≤1). Others have estimated similar values of whole-reach retention during storms (~40%) and attributed it to significant in-stream N demand during stormflows despite shorter water residence time (Bernal et al., 2019). Since low, moderate, and large storms can mobilize different quantities of sediment in the watershed of varying sources and sizes, it is likely that storm size will ultimately modulate the contribution of water column uptake during storm events to whole-reach N retention.

Particle size and chemical analysis in our experiments revealed important differences among sediment sources that can affect water column N uptake. Based on our limited particle size analysis, streambed sediments contained a greater proportion of sand-sized particles than the other two sources, as well as a higher contribution of coarse particles to sediment surface area. Nonetheless, it is important to note that source-specific proportions of fine and coarse materials in suspended sediments will vary as a function of stream discharge (Slattery and Burt, 1998), and their proper characterization was beyond the scope of our study. In our study, we purposely assessed similar SSC gradients of fine and coarse fractions of each sediment source to independently test the effects of increasing surface area on water column N uptake—*i.e.,* given equal SSC, fine particles will provide more surface area than coarse ones. Our results showed no statistical evidence of the expected positive effects of sediment surface area (clay/silt vs. sand) on water column N uptake; although we generally observed similar or greater sediment-specific N uptake rates in clay/silt microcosms than in those with sand-sized particles, with the one exception for assimilatory uptake in stream banks sediments. However, due to methodological difficulties when adding sediment to the microcosms, clay/silt microcosms for stream

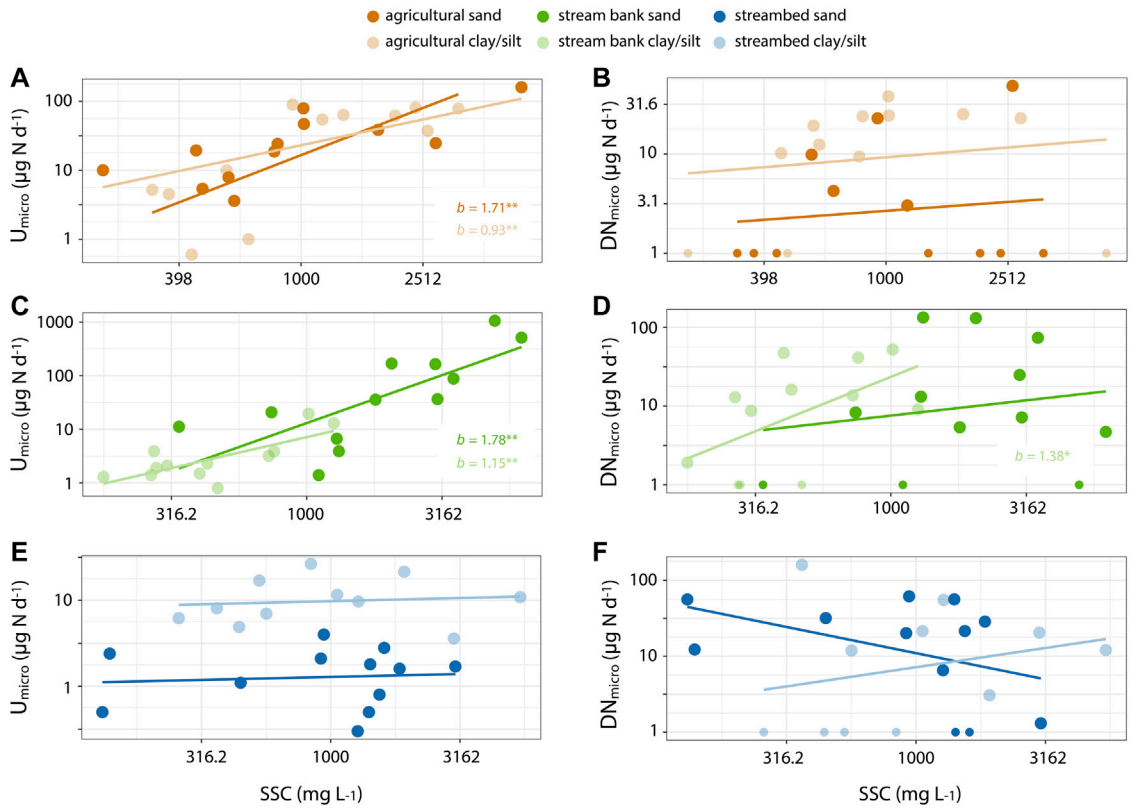

FIGURE 5
Log-log relationships between suspended sediment concentration (SSC) and microcosm-specific rates of assimilatory uptake **(A,C,E)** and denitrification **(B,D,F)** for each sediment source and size. Color legend is consistent with previous figures. Slope values and significance [(blank) $p > 0.05$; *$p < 0.05$; **, $p < 0.01$; ***$p < 0.001$] are indicated in each panel.

bank sediments covered a much narrower range than those with stream bank sand, 177–1,260 and 337–6,216 mg·L^{-1}, respectively. This was unintentional and it was not the case for the other two sediment sources. But it is plausible that the higher N uptake rates in stream bank sand was due to a lower SSC range being tested for the clay/silt fraction.

Beyond differences in particle size, C and N content varied significantly among sediment sources, and they seem to be relevant factors influencing microbial colonization and uptake in suspended sediments. We found higher C:N ratios in streambed sediments than in stream bank or agricultural sediments, along with generally higher C:N ratios of coarser sediments within each source. These results are similar to the negative relationship between particle size and C:N ratios reported by Sinsabaugh and Linkins (1990) in a forested, New England stream and by Zhang et al. (2021), who also suggested that high C:N can constrain bacterial colonization and denitrifying functional genes. Indeed, agricultural soils and stream bank sediments in our study with lower C:N ratios contained higher denitrifying bacterial gene (*nosZ*) abundances than streambed sediments. This is also concordant with the higher *nosZ* abundance in suspended sediments of WCC during one of the highest stormflow on record that very likely mobilized large amounts of hillslope sediment (Kan 2018). However, differences in *nosZ* gene abundance across sediment sources were completely opposite to those of measured denitrification rates, which were highest for streambed suspended sediments. We speculate that this mismatch can be partly explained by the irregular presence and high variation of water column denitrification in streambed sediments, which showed both the highest DN_{sed} values and the largest amount of non-detectable rates compared to the other two sediment sources. High variation in water column denitrification rates have been previously observed in suspended sediments of streambed origin across rivers of contrasting size (Reisinger et al., 2016). Recent work has emphasized the role of heterogeneous anoxic/hypoxic microsites on the activation of anaerobic microbial activity in suspended sediments (Zhu et al., 2018; Schulz et al., 2022). We contend that large variation in denitrification

TABLE 2 Results of two separate ANCOVA models testing the effects of sediment source, size and suspended sediment concentration (SSC) on assimilatory uptake (U_{micro}) and denitrification (DN_{micro}) rates, respectively. All data were log_{10}-transformed prior to the analysis. Bold values indicate significant ANCOVA effects as stated in the table caption.

Factors and covariate	Df	Mean sum sq	F-value	*p*-value
Assimilatory uptake (U_{micro})				
SSC	**1**	**12.8**	**61**	**<0.001**
Sediment Source	**2**	**3.3**	**15.6**	**<0.001**
Sediment Size	1	0.4	1.9	0.165
SSC:source	**2**	**3.6**	**17.3**	**<0.001**
SSC:size	1	0.4	1.9	0.164
Residuals	61	0.2		
Denitrification (DN_{micro})				
SSC	1	0.2	0.4	0.507
Sediment Source	2	0.9	0.9	0.379
Sediment Size	1	0.2	0.4	0.505
SSC:source	2	0.5	1.0	0.362
SSC:size	1	1.7	3.5	0.066
Residuals	61	0.5		

could be attributed to most denitrifying bacteria being facultative anaerobes that can respond rapidly to small-scale and/or short-term heterogeneity in oxygen availability.

Water column NO_3^- uptake varies considerably across rivers of different size, SSC, and N availability [from 0.001 to 363 mg·N·m^{-3} h^{-1} in Reisinger et al., (2015)]. In our microcosm study, water column NO_3^- uptake (U_{micro} + DN_{micro}) showed a narrower range (from 0.1 to 177 mg·N·m^{-3}·h^{-1}), with a high contribution of denitrification, when present, to water column NO_3^- uptake (mean ± SD: 41.7 ± 4.4%). Assuming a stream depth of 1 m, we estimated that microcosm-specific denitrification represented a mean areal rate of 3.3 ± 0.6 mg·N·m^{-2}·h^{-1}, which is very similar to median areal denitrification rates (1.7 mg·N·m^{-2}·h^{-1}) measured in multiple rivers during the warmest months of the year (Piña-Ochoa and Álvarez-Cobelas, 2006). Areal denitrification rates in our microcosm study ranged from 0 to 26.5 mg·N·m^{-2}·h^{-1}, which is comparably higher than the range found by Reisinger et al. (2016) of 0–4.9 mg·N·m^{-2}·h^{-1} in rivers with lower SSC and N availability. In contrast, we found similar sediment-specific denitrification rates to those reported by Reisinger et al. (2016). Therefore, these comparisons most likely highlight the positive effects of high SSC on water column N uptake, as SSCs in our microcosm study were much higher than in any of these previous studies. On the other hand, other studies using microcosms with even higher SSC (up to 20 g·L^{-1}) and 25-day incubations observed tenfold lower rates of water column denitrification than in our study (Liu et al., 2013; Jia et al., 2016). This could be due to the also ten times lower mean number of denitrifying genes they found compared to *nosZ* abundances in our study, or due to the effects of much different incubation times on net N processes. Overall, our results suggest that even during periods of high SSC associated with stormflow conditions, water column denitrification seems to be highly irregular and variable, akin to the patterns previously observed for benthic denitrification. Comparatively, assimilatory uptake in our study responded more strongly to *a priori* predictors of biological activity in suspended sediment such as %OM or increasing SSC than denitrification.

Consideration of other uptake processes besides denitrification is critical within the context of N removal in the water column. Assimilatory uptake can remove a comparatively larger amount of NO_3^- from the water column, which slows downstream N export and can eventually be permanently removed *via* remineralization and coupled nitrification/denitrification (Mulholland et al., 2004; Arango et al., 2008; Tank et al., 2018). Both microcosm- and sediment-specific assimilatory uptake rates were higher for stream bank and agricultural soils than for streambed sediments. When comparing assimilatory uptake rates in clay/silt and sand fractions for each sediment source, only streambed sediments showed significant effects of the greater surface area associated with fine sediments, even though we expected a similar result across all sediment sources. One explanation is that the larger median particle size in streambed sediments (Figure 1) may have resulted in larger differences in surface area between the clay/silt and sand fractions. In other words, the coarse fraction of agricultural and stream bank sediments in our microcosms most likely contained on average smaller sediment particles than the coarse fraction of streambed sediments. The effects of smaller sediment particles (i.e., greater surface area) in agricultural and stream bank sediments could also explain the higher intercepts in the %C-U_{sed} relationships for agricultural and stream bank sources compared to that of streambed sediments (Figure 4).

Similarly, the effects of increasing SSC and surface area on assimilatory N uptake were also much more notable for agricultural and stream bank sources. However, power exponents (i.e., scaling coefficients) in Figure 5 were similar or greater than 1, much higher than the expected ⅔ power exponents for sediment surface area to volume scaling, which indicates that assimilatory N uptake in the water column increased out of proportion with SSC and was likely also depending on additional factors beyond sediment surface area. Further assessment of scaling relationships between increasing SSC and water column uptake is necessary to improve the ability of existing watershed models to characterize N removal during storm events along stream watersheds.

In summary, results from our study suggest that the role of water column uptake on whole-reach N removal may be greater in watersheds with a high presence of agricultural and stream bank sediments that can be mobilized by storm events. Our microcosm study indicates that assimilatory N uptake is positively and nonlinearly related to increasing SSC with varying scaling coefficients depending on sediment sources and size. In our watershed, agricultural soils and stream bank sediments with higher C and N content than streambed sediments, and greater surface area per sediment load, were more reactive to increasing SSC. Accordingly, the contribution of water column N uptake to N retention at the watershed scale may be positively related to the contribution of agricultural and/or stream banks sources to stormflow sediment loads. Our microcosm study provides valuable data on how water column N uptake may scale with increasing storm size; however, more research on how these scaling relationships change across streams of contrasting land use, size, and channel forms is necessary to improve our understanding of water column processes at the watershed scale.

Data availability statement

The datasets analyzed for this study are deposited in the open-access repository, https://github.com/evabacmeister/microcosm2022.

Author contributions

EB, JK, SI, EP, and MP designed the microcosm experiments. EB, SB, and EP collected sediment samples and performed the microcosms experiments. EB and MP analyzed the data and wrote the manuscript with contributions from EP, JK, SB, and SI.

Funding

This research was financially supported by the US Department of Agriculture grant NIFA-12912936 to MP, SI, and JK. Part of the data used for the study design and decision-making of sediment collection sites was collected with the financial support of the National Science Foundation grant DEB-155706 to M Peipoch and JK.

Acknowledgments

The authors are grateful to J. Carroll and L. Zgleszewski for their laboratory assistance.

Conflict of interest

The authors declare that the research was conducted in the absence of any commercial or financial relationships that could be construed as a potential conflict of interest.

Publisher's note

References

APHA Standard (1985). Methods for examination of water and waste. Available at https://www.scirp.org/(S(lz5mqp453edsnp55rrgjct55))/reference/ReferencesPapers.aspx?ReferenceID=373727.

Arango, C. P., Tank, J. L., Johnson, L. T., and Hamilton, S. K. (2008). Assimilatory uptake rather than nitrification and denitrification determines nitrogen removal patterns in streams of varying land use. *Limnol. Oceanogr.* 53, 2558–2572. doi:10.4319/lo.2008.53.6.2558

Bernal, S., Lupon, A., Wollheim, W. M., Sabater, F., Poblador, S., and Martí, E. (2019). Supply, demand, and in-stream retention of dissolved organic carbon and nitrate during storms in Mediterranean forested headwater streams. *Front. Environ. Sci.* 7, 60. doi:10.3389/fenvs.2019.00060

Cashman, M. J., Gellis, A., Sanisaca, L. G., Noe, G. B., Cogliandro, V., and Baker, A. (2018). Bank-derived material dominates fluvial sediment in a suburban Chesapeake bay watershed. *River Res. Appl.* 34 (8), 1032–1044. doi:10.1002/rra.3325

Craig, L. S., Palmer, M. A., Richardson, , D. C., Filoso, S., Bernhardt, E. S., Bledsoe, B. P., et al. (2008). Stream restoration strategies for reducing river nitrogen loads. *Front. Ecol. Environ.* 6, 529–538. doi:10.1890/070080

Dodds, W. K., Burgin, A. J., Marcarelli, A. M., and Strauss, E. A. (2017). "Nitrogen transformations," in *Methods in stream ecology: Third edition*.

Dodds, W. K., and Smith, V. H. (2016). Nitrogen, phosphorus, and eutrophication in streams. *Inland Waters* 6, 155–164. doi:10.5268/iw-6.2.909

Gardner, J. R., and Doyle, M. W. (2018). Sediment–water surface area along rivers: Water column versus benthic. *Ecosystems* 21, 1505–1520. doi:10.1007/s10021-018-0236-2

Gellis, A. C., and Gorman-Sanisaca, L. (2018). Sediment fingerprinting to delineate sources of sediment in the agricultural and forested Smith Creek

watershed, Virginia, USA. *J. Am. Water Resour. Assoc.* 54, 1197–1221. doi:10.1111/1752-1688.12680

Gellis, A. C., Hupp, C. R., Pavich, M. J., Landwehr, J. M., Banks, W. S. L., Hubbard, B. E., et al. (2009). *Sources, transport, and storage of sediment at selected sites in the chesapeake bay watershed*. Reston, VA: USGS Publications Warehouse.

Gellis, A. C., and Mukundan, R. (2013). Watershed sediment source identification: Tools, approaches, and case studies. *J. Soils Sediments* 13, 1655–1657. doi:10.1007/s11368-013-0778-z

Gellis, A. C., and Noe, G. B. (2013). Sediment source analysis in the linganore Creek watershed, Maryland, USA, using the sediment fingerprinting approach: 2008 to 2010. *J. Soils Sediments* 13, 1735–1753. doi:10.1007/s11368-013-0771-6

Henry, S., Bru, D., Stres, B., Hallet, S., and Philippot, L. (2006). Quantitative detection of the nosZ gene, encoding nitrous oxide reductase, and comparison of the abundances of 16S rRNA, narG, nirK, and nosZ genes in soils. *Appl. Environ. Microbiol.* 72, 5181–5189. doi:10.1128/aem.00231-06

Inamdar, S., Johnson, E., Rowland, R., Warner, D., Walter, R., and Merritts, D. (2018). freeze–thaw processes and intense rainfall: The one-two punch for high sediment and nutrient loads from mid-atlantic watersheds. *Biogeochemistry* 141, 333–349. doi:10.1007/s10533-017-0417-7

Jia, Z., Liu, T., Xia, X., and Xia, N. (2016). Effect of particle size and composition of suspended sediment on denitrification in river water. *Sci. Total Environ.* 541, 934–940. doi:10.1016/j.scitotenv.2015.10.012

Jiang, G., Lutgen, A., Mattern, K., Sienkiewicz, N., Kan, J., and Inamdar, S. (2020). Streambank legacy sediment contributions to suspended sediment-bound nutrient yields from a mid-Atlantic, Piedmont watershed. *J. Am. Water Resour. Assoc.* 56, 820–841. doi:10.1111/1752-1688.12855

Jones, C. M., Graf, D. R. H., Bru, D., Philippot, L., and Hallin, S. (2013). The unaccounted yet abundant nitrous oxide-reducing microbial community: A potential nitrous oxide sink. *Isme J.* 7, 417–426. doi:10.1038/ismej.2012.125

Kan, J. (2018). Storm events restructured bacterial community and their biogeochemical potentials. *J. Geophys. Res. Biogeosci.* 123, 2257–2269. doi:10.1029/2017jg004289

Karwan, D. L., Pizzuto, J. E., Aalto, R., Marquard, J., Harpold, A., Skalak, K., et al. (2018). Direct channel precipitation and storm characteristics influence short-term fallout radionuclide assessment of sediment source. *Water Resour. Res.* 54, 4579–4594. doi:10.1029/2017wr021684

Liu, T., Xia, X., LiuS.Mou, X., and Qiu, Y. (2013). Acceleration of denitrification in turbid rivers due to denitrification occurring on suspended sediment in oxic waters. *Environ. Sci. Technol.* 47, 4053–4061. doi:10.1021/es304504m

Lutgen, A., Jiang, G., Sienkiewicz, N., Mattern, K., Kan, J., and Inamdar, S. (2020). Nutrients and heavy metals in legacy sediments: Concentrations, comparisons with upland soils, and implications for water quality. *J. Am. Water Resour. Assoc.* 56, 669–691. doi:10.1111/1752-1688.12842

Menzel, D. W., and Vaccaro, R. F. (1964). The measurement of dissolved organic and particulate carbon in seawater1. *Limnol. Oceanogr.* 9, 138–142. doi:10.4319/lo.1964.9.1.0138

Mulholland, P. J., Hall, R. O., Sobota, D. J., Dodds, W. K., Findlay, S. E. G., Grimm, N. B., et al. (2009). Nitrate removal in stream ecosystems measured by 15N addition experiments: Denitrification. *Limnol. Oceanogr.* 54, 666–680. doi:10.4319/lo.2009.54.3.0666

Mulholland, P. J., Tank, J. L., Sanzone, D. M., Wollheim, W. M., Peterson, B. J., Webster, J. R., et al. (2000). Nitrogen cycling in a forest stream determined by a 15 N tracer addition. *Ecol. Monogr.* 70, 471–493. doi:10.2307/2657212

Mulholland, P. J., Valett, H. M., Webster, J. R., Thomas, S. A., Cooper, L. W., Hamilton, S. K., et al. (2004). Stream denitrification and total nitrate uptake rates measured using a field ^{15}N tracer addition approach. *Limnol. Oceanogr.* 49, 809–820. doi:10.4319/lo.2004.49.3.0809

Nielsen, L. P. (1992). Denitrification in sediment determined from nitrogen isotope pairing. *FEMS Microbiol. Ecol.* 86, 357–361. doi:10.1111/j.1574-6941.1992.tb01771.x

Noe, G. B., Cashman, M. J., Skalak, K., Gellis, A., Hopkins, K. G., Moyer, D., et al. (2020). Sediment dynamics and implications for management: State of the science from long-term research in the Chesapeake Bay watershed, USA. *WIREs Water* 7, e1454. doi:10.1002/wat2.1454

Peipoch, M., Gacia, E., Pastor, A., Ribot, M., Riera, J. L., Sabater, F., et al. (2014). Intrinsic and extrinsic drivers of autotrophic nitrogen cycling in stream ecosystems: Results from a translocation experiment. *Limnol. Oceanogr.* 59, 1973–1986. doi:10.4319/lo.2014.59.6.1973

Peterson, B. J., Wollheim, W. M., Mulholland, P. J., Webster, J. R., Meyer, J. L., Tank, J. L., et al. (2001). Control of nitrogen export from watersheds by headwater streams. *Science* 292, 86–90. doi:10.1126/science.1056874

R Core Team (2013). R A language and environment. Available at https://www.scirp.org/(S(i43dyn45teexjx455qlt3d2q))/reference/ReferencesPapers.aspx?ReferenceID=1787696.

Reisinger, A. J., Tank, J. L., Rosi-Marshall, E. J., Hall, R. O., and Baker, M. A. (2015). The varying role of water column nutrient uptake along river continua in contrasting landscapes. *Biogeochemistry* 125, 115–131. doi:10.1007/s10533-015-0118-z

Reisinger, A. J., Tank, J. L., Hall, R. O., Rosi, E. J., Baker, M. A., and Genzoli, L. (2021). Water column contributions to the metabolism and nutrient dynamics of mid-sized rivers. *Biogeochemistry* 153, 67–84. doi:10.1007/s10533-021-00768-w

Reisinger, A. J., Tank, J. L., Hoellein, T. J., and Hall, R. O. (2016). Sediment, water column, and open-channel denitrification in rivers measured using membrane-inlet mass spectrometry. *J. Geophys. Res. Biogeosci.* 121, 1258–1274. doi:10.1002/2015jg003261

Schlesinger, W. H. (2009). On the fate of anthropogenic nitrogen. *Proc. Natl. Acad. Sci. U. S. A.* 106, 203–208. doi:10.1073/pnas.0810193105

Schulz, G., Sanders, T., Beusekom, J. E. E. V., Voynova, Y. G., Schöl, A., and Dähnke, K. (2022). Suspended particulate matter drives the spatial segregation of nitrogen turnover along the hyper-turbid Ems estuary. *Biogeosciences* 19, 2007–2024.

Shoda, M. E., Sprague, L. A., Murphy, J. C., and Riskin, M. L. (2019). Water-quality trends in U.S. rivers, 2002 to 2012: Relations to levels of concern. *Sci. Total Environ.* 650, 2314–2324. doi:10.1016/j.scitotenv.2018.09.377

Sinsabaugh, R. L., and Linkins, A. E. (1990). Enzymic and chemical analysis of particulate organic matter from a boreal river. *Freshw. Biol.* 23, 301–309. doi:10.1111/j.1365-2427.1990.tb00273.x

Slattery, M. C., and Burt, T. P. (1998). Particle size characteristics of suspended sediment in hillslope runoff and stream flow. *Earth Surf. Process. Landf.* 22, 705–719. doi:10.1002/(sici)1096-9837(199708)22:8<705::aid-esp739>3.0.co;2-6

Tank, J. L., Marti, E., Riis, T., von Schiller, D., Reisinger, A. J., Dodds, W. K., et al. (2018). Partitioning assimilatory nitrogen uptake in streams: An analysis of stable isotope tracer additions across continents. *Ecol. Monogr.* 88, 120–138. doi:10.1002/ecm.1280

Weiss, R. F. (1970). The solubility of nitrogen, oxygen and argon in water and seawater. *Deep Sea Res. Oceanogr. Abstr.* 17, 721–735.

Wollheim, W. M., Bernal, S., Burns, D. A., Czuba, J. A., Driscoll, C. T., Hansen, A. T., et al. (2018). river network saturation concept: Factors influencing the balance of biogeochemical supply and demand of river networks. *Biogeochemistry* 141, 503–521. doi:10.1007/s10533-018-0488-0

Wollheim, W. M., Mulukutla, G. K., Cook, C., and Carey, R. O. (2017). Aquatic nitrate retention at river network scales across flow conditions determined using nested *in situ* sensors. *Water Resour. Res.* 53, 9740–9756. doi:10.1002/2017wr020644

Wood, P. J., and Armitage, P. D. (1997). Biological effects of fine sediment in the lotic environment. *Environ. Manage.* 21, 203–217. doi:10.1007/s002679900019

Xia, X., Liu, T., Yang, Z., Michalski, G., Liu, S., Jia, Z., et al. (2017). Enhanced nitrogen loss from rivers through coupled nitrification-denitrification caused by suspended sedimentT1. *Sci. Total Environ.* 579, 47–59. doi:10.1016/j.scitotenv.2016.10.181

Xia, X., Zhang, S., Li, S., Zhang, L., Wang, G., Zhang, L., et al. (2018). The cycle of nitrogen in river systems: Sources, transformation, and flux. *Environ. Sci. Process. Impacts* 20, 863–891. doi:10.1039/C8EM00042E

Zhu, W., Wang, C., Hill, J., He, Y., Tao, B., Mao, Z., et al. (2018). A missing link in the estuarine nitrogen cycle?: Coupled nitrification-denitrification mediated by suspended particulate matter. *Sci. Rep.* 8, 2282–2310. doi:10.1038/s41598-018-20688-4